Chronology of colluvial apron deposition within Canada del Buey, Pajarito Plateau, New Mexico

Kenneth Lepper, Kelly Crowell, and Cathy Wilson

New Mexico Geology, v. 33, n. 1 pp. 3-8, Print ISSN: 0196-948X, Online ISSN: 2837-6420.
https://doi.org/10.58799/NMG-v33n1.3

This page is intentionally left blank to maintain order of facing pages.

Chronology of colluvial apron deposition within Cañada del Buey, Pajarito Plateau, New Mexico

Kenneth Lepper, Optical Dating and Dosimetry Lab, Department of Geosciences, North Dakota State University, Fargo, North Dakota 58108-6050, ken.lepper@ndsu.edu; *Kelly Crowell*, Portage Inc., Los Alamos, New Mexico 87544;
Cathy Wilson, Earth Systems Observations, Earth and Environmental Science Division, Los Alamos National Laboratory, EES-14, Los Alamos, New Mexico 87545

Abstract

This investigation uses optically stimulated luminescence (OSL) dating to examine the chronology of colluvial apron development and to help constrain long-term process rates within the mesa and canyon systems of the Pajarito Plateau in north-central New Mexico. In addition to ages, the OSL data provide insight into the dynamic interactions of surface processes within the mesa and canyon systems. Our results can be interpreted to suggest that foot-slope deposits within Cañada del Buey represent a complex interplay of depositional processes in which eolian inputs from outside of the Pajarito Plateau play a role. Depositional ages, both on the mesa top and in foot slopes, record episodic inputs to the system in the late Pleistocene, middle Holocene, and late Holocene. These periods correlate well to eolian activity and significant climatic events in the Southern Plains and desert Southwest.

Introduction

The Pajarito Plateau forms the eastern and southeastern flanks of the Valles caldera in the Jemez Mountains of north-central New Mexico (Fig. 1). The rocks associated with the plateau are composed of volcanic deposits, predominantly basalt flows and ignimbritic tuffs. The ignimbrites were erupted from the caldera in two principal catastrophic events occurring approximately 1.6 and 1.2 Ma (Izett and Obradovich 1994; Phillips et al. 2007). Over the past 1.2 m.y., tributary streams of the Rio Grande have dissected the plateau into mesa-like promontories by headward erosion of braided stream systems (Reneau 1995). Within the canyon complex, colluvial aprons form transitional slopes between the steep-walled promontories or mesas and canyon stream floodplains. In the area of Los Alamos National Laboratory (LANL), these mesas and the intervening streams that carved them trend to the east and southeast.

Rates and processes of mesa erosion and colluviation are of interest to custodians of the lands in and around LANL and to drylands geomorphologists in general. Common environmental monitoring techniques like stream gaging are used to assess short-term erosion rates (years to decades) from the mesas; however, longer-term erosion rates (hundreds to thousands of years) and the complex interaction of surface processes that affect mesa erosion and colluviation within the canyons on longer timescales are not well understood. Reneau (1995) suggests that edge retreat mesa erosion occurs via block fall and deep-seated landslides. However, in addition to rock debris from these significant mass-wasting events, mesa foot slopes include finer-grained sediments with colluvial, alluvial, and eolian origins (Drakos et al. 2007).

An intriguing aspect of the mesa and canyon systems in the area is geomorphic asymmetry of the colluvial aprons, or foot slopes, on either side of the mesas. To the north and northeast of the mesas, colluvial aprons have gentler slopes and extend farther from the inferred mesa base than on the south and southwest sides of the mesas (Figs. 2 and 3). Slope aspect could have an influence on block fall mesa erosion due to differences in thermal expansion/contraction or frost wedging acting disproportionately on opposite-facing slopes. However, based on our field reconnaissance, the observed asymmetry in colluvial aprons does not appear to be directly attributable to differences in block fall. Colluvial aprons beneath southwest-facing mesa walls are generally smaller, but appear to have similar, if not greater, contributions from block fall as compared to colluvial aprons developed beneath northeast-facing mesa walls. Burnett et al. (2008) document similar side-slope asymmetry between north-facing and south-facing cliffs in a northeastern Arizona study area where sandstones were the dominant cliff-forming rock type. They found that topographically induced microclimatic variations contributed significantly to side-slope asymmetry in their study area.

The primary objective of this investigation was to obtain optically stimulated luminescence (OSL) ages for sediments from mesa tops and adjacent colluvial aprons to establish a chronology for constraining long-term process rates in the mesa and canyon systems. In this study, we have examined one particular mesa-canyon pair, Mesita del Buey and Cañada del Buey (Fig. 2), to gain insight into the rates and variations in geologic surface processes that contribute to colluvial-apron development.

Sampling

The sediment samples examined in this investigation were collected as adjacent pairs (within 15–30 cm or 6–12 inches from each other) of vertical piston cores in 2.54 cm diameter plastic liners. One core from each pair was shielded from light at all times and subsampled for OSL dating. Soil stratigraphic descriptions were made on the companion cores and used as the basis for selecting the OSL sample horizons. Two pairs of cores were collected from the top of Mesita del Buey to provide age control and reference data as the potential source material for the colluvial aprons (Fig. 2; Table 1).

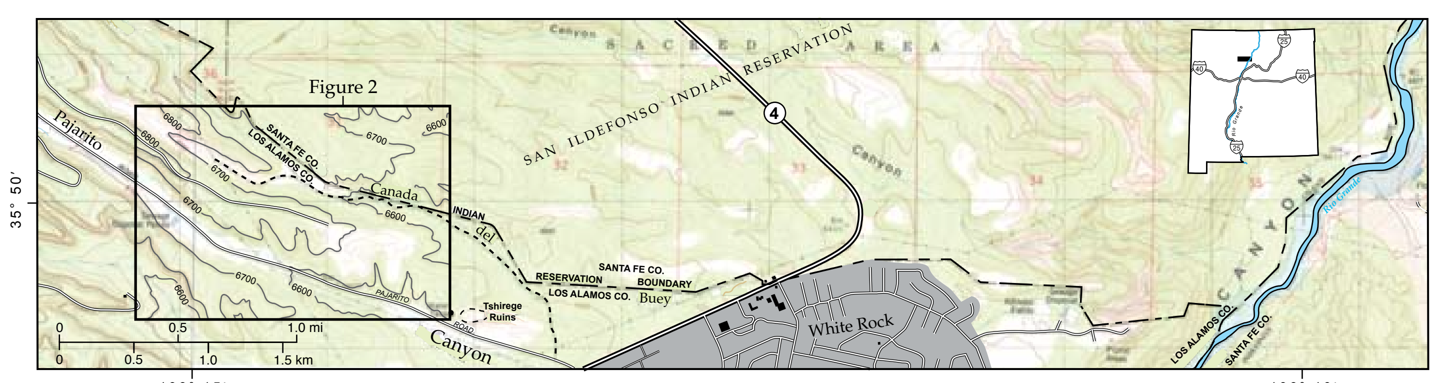

FIGURE 1—Topographic map of parts of the White Rock and Frijoles 7.5-min quadrangles, showing the mesas and canyons of the Pajarito Plateau, the Rio Grande, and the area of Figure 2 (outlined).

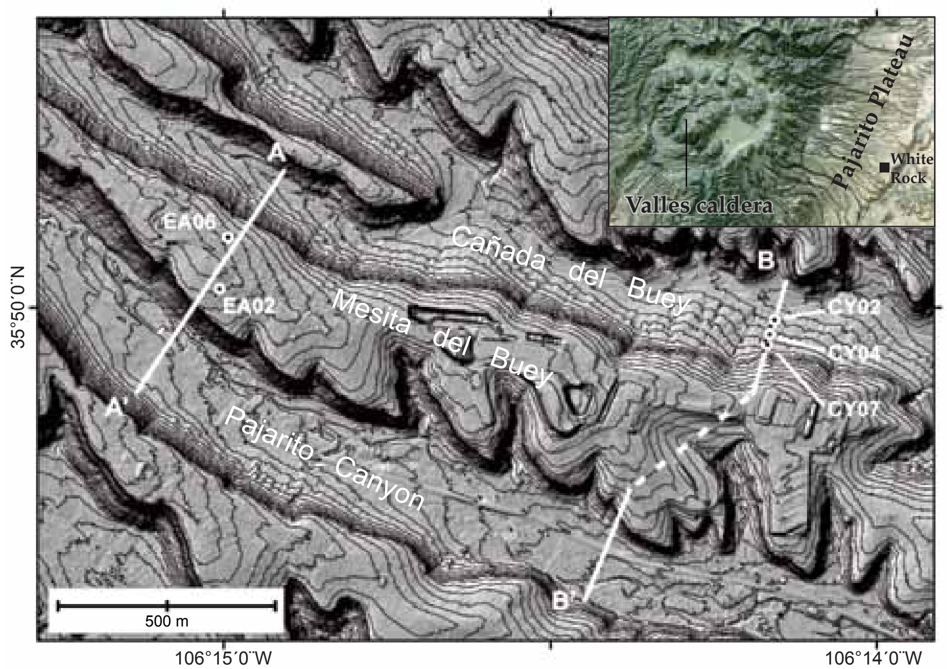

FIGURE 2—Airborne laser mapping-derived shaded-relief imagery of several mesas and intervening canyons of the Pajarito Plateau (for additional discussion of data set see Carey and Cole 2002). Core sites are indicated by symbols. Transect lines correspond to the topographic profiles shown in Figure 3. Inset shows Pajarito Plateau east and southeast of the Valles caldera.

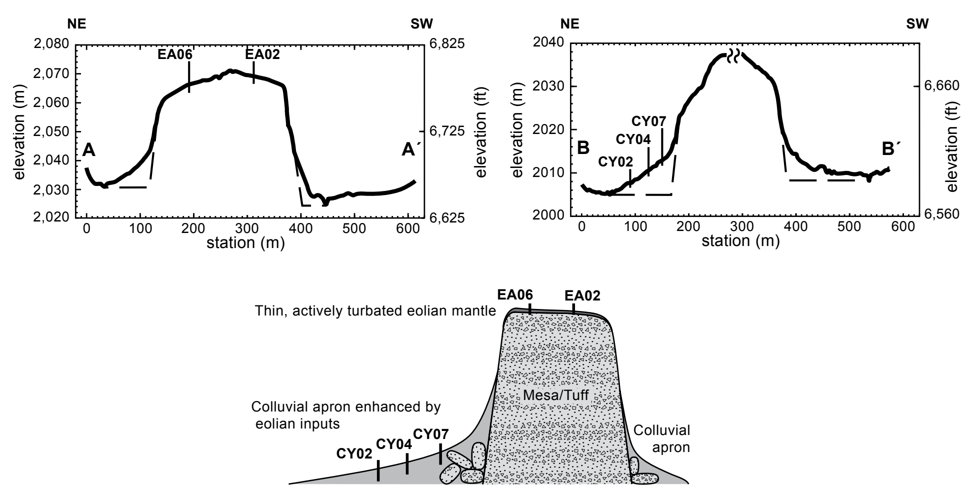

FIGURE 3—Topographic profiles from mesa top down to stream level taken approximately perpendicular to the trend of Mesita del Buey. The location of the transects A–A′ (top left) and B–B′ (top right) are indicated in Figure. 2. These profiles demonstrate the asymmetry of the foot-slope deposits on either side of Mesita del Buey. The lower panel is a conceptualized diagram meant to illustrate the contextual relationship of the samples and the geomorphic asymmetry on either side of the mesas.

TABLE 1—Sample core coordinates and core top elevations.

Sample core	Companion/ description core	Longitude (W)	Latitude (N)	Elevation (m)	Elevation (ft)
CY02	CY01	106.23597	35.83307	2,007.8	6,587.3
CY04	CY03	106.23609	35.83277	2,010.7	6,596.8
CY07	CY06	106.23616	35.83256	2,012.9	6,604.0
EA02	EA01	106.25012	35.83371	2,067.9	6,784.4
EA06	EA05	106.24991	35.83478	2,067.2	6,782.2

Metric elevations were obtained by sampling the DEM used as the basis of Figure 2.

The surface of Mesita del Buey has been heavily influenced by anthropogenic activities; however, the sites selected for the two mesa-top cores were thought to be undisturbed by modern anthropogenic activities based on available LANL records and field reconnaissance. Three pairs of cores were collected from foot-slope deposits in Cañada del Buey along an approximately linear transect from mesa wall to stream that was perpendicular to the general trend of the mesa (Fig. 2; Table 1). Although the original sampling strategy targeted colluvial aprons on either side of Mesita del Buey, the high gradient and abundance of surficial rock debris in colluvial aprons on the southwestern flanks of Mesita del Buey severely limited site selection and accessibility by coring equipment; therefore, cores were not collected from foot slopes in Pajarito Canyon.

The shielded cores were subsampled in the light-controlled Luminescence Geochronology Laboratory at LANL by cutting through the core liner and the sediments within. Each OSL sample was a 5-cm segment of the core. Canyon foot-slope cores were sampled at multiple depth intervals. The OSL samples were then repackaged and transported to the Optical Dating and Dosimetry Lab at North Dakota State University for further processing and OSL dating measurements.

Methods

Clean quartz sand in the size fraction 90–250 μm (very fine to medium sand) was obtained by typical luminescence dating sample preparation procedures, which include wet sieving, digestion of organic matter by hydrogen peroxide, aggressive treatment with hydrofluoric (HF) acid to break down feldspar grains and etch the surface of quartz grains, as well as hydrochloric (HCl) acid and Na-pyrophosphate treatments to remove precipitates and particulates. After drying, the quartz grains were attached to aliquots for OSL measurements using a non-luminescent medical adhesive.

All measurements and irradiations were conducted using a Risø DA-15 automated TL/OSL reader system. The system is equipped with a $^{90}Sr/^{90}Y$ beta-source that irradiated at a rate of 0.132 Gy/s, a blue diode array (OSL; 470 ± 30 nm), an EMI model 9235QA PMT, and a 48-position sample carousel. Stimulated luminescence was measured in the UV emission range (5 mm Hoya U-340) for all data sets in this report.

Age data were collected using OSL SAR (single aliquot regeneration) procedures (Murray and Wintle 2000; Wintle and Murray 2006). The experimental sequence for the SAR measurements is given in Table 2. Dose response calibration was conducted for every aliquot, and equivalent doses (D_e) were determined by interpolation from linear local slope approximations. D_e data sets were filtered before dose distribution analysis using the criteria described in Lepper et al. (2003). Dose distribution characteristics including symmetry/asymmetry

TABLE 2—Sequence of experimental procedures used for OSL SAR data collection.

Sequence of procedures		Parameter definitions
Preheat		10 s @ 160˚C
Measure natural signal		OSL 50 s @ 125˚C
Irradiate test dose		Sample specific
Preheat		10 s @ 160˚C
Measure test dose		OSL 50 s @ 125˚C
4 iterations	Irradiate calibration* dose	Sample specific
	Preheat	10 s @ 160˚C
	Measure calibration* dose	OSL 50 s @ 125˚C
	Irradiate test dose	Sample specific
	Preheat	10 s @ 160˚C
	Measure test dose	OSL 50 s @ 125˚C
Irradiate check** dose		Sample specific
Preheat		10 s @ 160˚C
Measure check** dose		OSL 50 s @ 125˚C
Irradiate test dose		Sample specific
Preheat		10 s @ 160˚C
Measure test dose		OSL 50 s @ 125˚C

*Referred to as regeneration dose in SAR procedure.
**Analogous to a dose recovery test preformed on every aliquot (discussed in Lepper et al. 2000 and 2003).

TABLE 3—Elemental concentrations from INAA and other dosimetric data.

Sample	K (ppm)	U (ppm)	Th (ppm)	H_2O content (%)	Sample depth (cm)
CY02A	33,544 ± 3,367	3.68 ± 1.21	11.21 ± 1.41	8 ± 3	4–9
CY02B	27,055 ± 2,681	3.58 ± 0.72	5.12 ± 0.63	10 ± 3	48–53
CY04A	30,127 ± 2,898	4.20 ± 0.92	4.50 ± 0.71	8 ± 3	14–19
CY04B	24,065 ± 2,289	3.71 ± 1.07	7.72 ± 1.51	10 ± 3	49–54
CY04C	23,639 ± 2,406	3.99 ± 0.79	3.79 ± 0.57	12 ± 3	95–100
CY07A	20,681 ± 1,979	4.17 ± 1.00	8.26 ± 1.06	10 ± 3	7–12
EA06	30,844 ± 3,036	3.74 ± 0.68	3.88 ± 0.49	5 ± 3	15–20

analysis (M/m – mean/median ratio; see Rowland et al. 2005; or supplement to Lepper et al. 2007) and data dispersion (υ; see Fuchs and Wagner 2003) were considered to inform age calculations.

Dose rates for samples in this investigation were determined from elemental concentrations of K, U, and Th by the method presented by Aitken (1998). Elemental analysis was obtained via instrumental neutron activation (INAA) at The Ohio State University research reactor (Table 3). The cosmic ray dose at depth was calculated using the equation developed by Prescott and Hutton (1988, 1994) adjusted for the local surface "hard" component (muon) dose rate of 0.30 mGy/a. An estimate of average water content over time for each sample is given in Table 3. This estimate is based on the soil/sediment texture and landscape position of the sample, as well as the geographic location of the sample site. A beta dose attenuation factor of 0.91 was used for sediment grains ranging in size from 90 to 250μm.

Results

Soil stratigraphy

Mesa-top soil profiles were capped with 15 cm (6 inches) of loose granular brown loam (A horizon). This surface layer appeared to be actively turbated and, because of its loose nature, is susceptible to mobilization by wind or slope-wash processes. The mesa-top cores exhibited clay loam and loamy clay B horizons that quickly graded into weathered tuff (Cr) by 50 cm (20 inches) depth in both cores. These soils have been interpreted to represent a regolith-derived soil (highly weathered tuff) with an eolian mantle (Eberly et al. 1995; Reneau et al. 1995, 1996; Drakos and Reneau 2007).

Foot-slope soil profiles were capped by a slightly thicker layer of loose granular brown loam (17–30 cm thick; A horizon). Similar to the mesa-top samples, the nature of these A horizons makes them susceptible to mobilization, most likely by slope wash, considering their respective landscape positions. The foot-slope profiles all exhibited two distinct subhorizons, within their B master horizons, which were much thicker than those observed on top of the mesa. These cores extended to depths of 88–106 cm (~3–3.5 ft) without encountering the presumed parent material, tuff or weathered tuff (C or Cr horizons). However, highly degraded and weathered tuff pebbles were observed in the lower B horizons of all the foot-slope cores. Additional soil profile descriptions from sites within Cañada del Buey can be found in Drakos et al. (2007).

General observations relevant to OSL dating: quartz sand content and OSL signal yield

After processing for OSL measurement, all samples except one yielded 200–500 mg of clean quartz sand in the grain size range 90–250 μm from 25 cm^3 of raw field sample. We consider this amount of quartz sand in itself to be evidence of external sediment inputs to the system because the tuff deposits of the Pajarito Plateau contain only a small fraction of sand-sized crystalline quartz (Broxton et al. 1995). We can compare the amount of quartz sand recovered in this study to our past work on locally derived floodplain deposits within the canyons of the Pajarito Plateau (Lepper et al. 2003; Gardner et al. 2003) in which we routinely processed 150–200 cm^3 of field sample (6–8× more material than in the current study) and generally obtained less than 200 mg of clean quartz sand. Only sample CY07B (the lower sample from the mesa-base core) was completely digested by HF, suggesting that the sample was derived primarily from weathered tuff (local).

OSL signal yield (dose normalized natural single-aliquot peak signal intensity) provides additional evidence that sediment grains in the canyon-slope deposits come from source areas outside of the Pajarito Plateau. The sample set from Mesita del Buey and Cañada del Buey has signal yields approximately two orders of magnitude greater than the locally derived floodplain sediments from Chupaderos Canyon, approximately 12 km (7.5 mi) from the present study site (Fig. 4; data for the comparison from Lepper et al. 2003). A plausible mechanism for delivering allochthonous quartz sand to the Pajarito Plateau is via eolian transport.

OSL dose distribution characteristics

Sediments from all the dated horizons within the canyon foot-slope cores exhibited symmetric dose distributions with

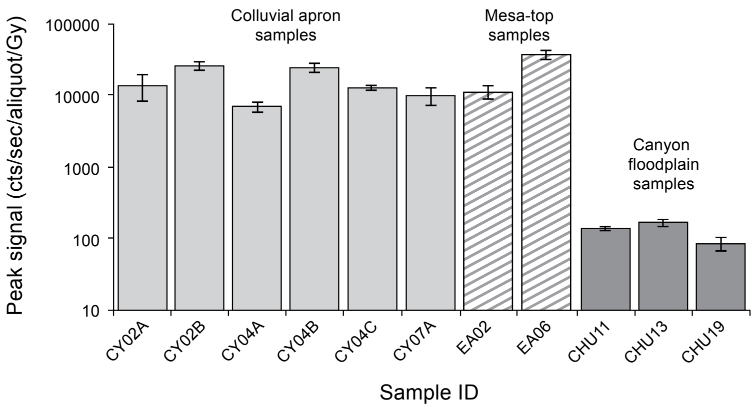

FIGURE 4—Natural signal yields for the prepared quartz samples in this investigation compared to three floodplain samples from Chupaderos Canyon (Lepper et al. 2003). A difference of approximately two orders of magnitude is indicated. The bars represent the average peak OSL signal and standard error of the "natural" signal, measured from 20* randomly selected aliquots of each field sample, scaled to one second of measurement time and divided by the sample's representative equivalent dose. *(Data were available from only three aliquots for sample CHU19.)

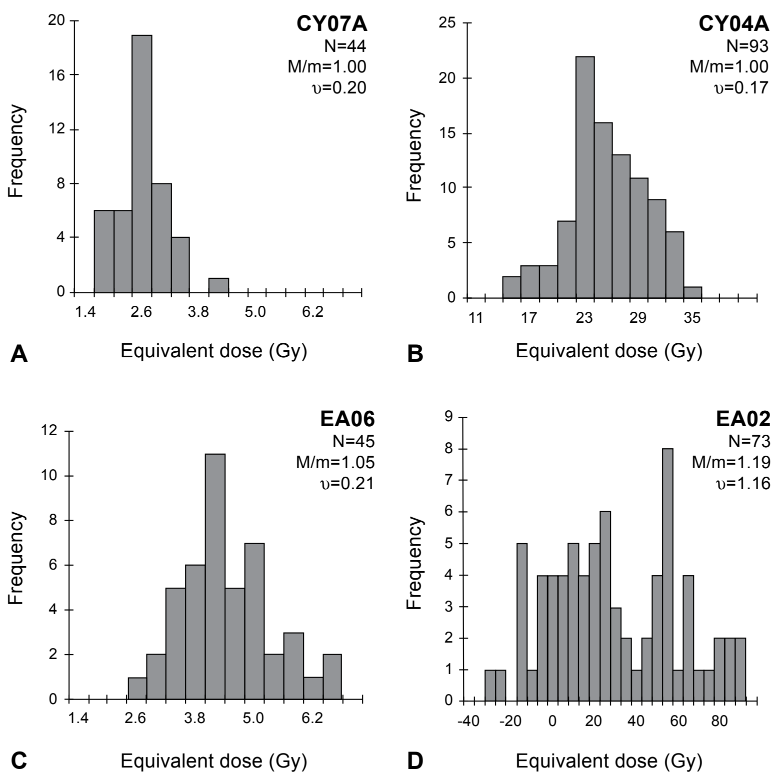

FIGURE 5—OSL SAR equivalent dose distributions from two representative foot-slope samples, panels (A) and (B), as well as the mesa-top sample EA06 (C), all of which are symmetric and have relatively low dispersion. Mesa-top sample EA02 (D), in contrast, exhibits extremely high data dispersion and, although not visually obvious, asymmetry as well.

moderate relative dispersion (M/m ratios of 0.99 to 1.01 and υ-values ranging generally from 0.17 to 0.26, with one value of 0.48; Fig. 5A and 5B; Table 4). We interpret these distribution characteristics as being consistent with well reset samples (M/m of ~1) that have undergone some degree of colluviation resulting in more D_e dispersion (moderate υ-values) than would normally be expected from eolian sediments. However, it should be kept in mind that the OSL analysis targeted quartz sand—the grains most likely to have been transported to the Pajarito Plateau by eolian processes due to their very low abundance in the tuffs.

Mesa-top sample EA06 exhibited a reasonably symmetric D_e distribution (M/m = 1.05) also with moderate dispersion (υ = 0.21) similar to the foot-slope samples (Fig. 5C; Table 4). In contrast, the D_e distribution of mesa-top sample EA02 (Fig. 5D) was asymmetric (M/m = 1.19) and highly dispersed (υ = 1.16). The dose distribution characteristics observed in sample EA02 could arise from vertical mixing: of eolian sediments deposited from more than one distinct event, of eolian sediments with weathered residuum, or of eolian sediments with disturbed surface materials. A high degree of eolian redistribution of modern sediments has been documented on the mesa surfaces (Environmental Surveillance Program 2003), and some areas of the mesa top also have been subjected to intensive anthropogenic disturbance.

OSL ages

All ages presented in Table 4 and Figure 6 were calculated based on the mean and standard error of the filtered D_e data sets. An age is not presented for sample EA02 due to extreme D_e data dispersion. Fuchs and Wagner (2003) have suggested that samples with large υ-values are not suitable for age calculations. We interpret the large asymmetry and extremely large relative dispersion of this sample's D_e data set to indicate a disturbed or naturally turbated soil at this coring site (discussed above; see also Bush and Feathers 2003).

A majority of the foot-slope core samples yielded ages ranging from 15.9 ± 1.3 ka to 11.4 ± 1.3 ka, suggesting a dominant late Pleistocene accumulation period along the foot slopes of sediments that were "well exposed to sunlight" before deposition. Other ages observed in the foot-slope cores were 6.3 ± 0.6 ka and 750 ± 80 yr, from the upper horizons of the mid-slope and mesa proximal landscape positions, respectively (Fig. 6). The dateable mesa-top sample, EA06, resulted in an age of 1,050 ± 100 yrs.

Discussion and interpretations

Based on the abundance of quartz in most samples, OSL signal yields, equivalent dose distribution characteristics, and the distinctive intervals of deposition, eolian contributions from sources outside the Pajarito Plateau appear to contribute to the development of colluvial aprons within Cañada del Buey. This interpretation is supported by past work (Reneau et al. 1995, 1996; Eberly et al. 1995; Drakos and Reneau 2007) documenting both the importance of eolian contributions to the soils of the Pajarito Plateau, and that significant eolian influxes to the system occurred in both the late Pleistocene and late Holocene. Additionally, because foot slopes in Cañada del Buey are broader, gentler, and contain a significantly greater abundance of fine-grained sediment than foot slopes in Pajarito Canyon, we interpret that the geomorphic asymmetry of foot-slope deposits on either side of Mesita del Buey could be attributable, at least in part, to enhanced eolian input to

TABLE 4—OSL SAR age results from quartz sand.

Sample ID	N[a]	M/m ratio[b]	υ[c]	Mean D_e (Gy)	Dose rate (Gy/ka)	OSL age
CY02A	84/94	1.01	0.48	54.67 ± 2.84	4.81 ± 0.43	11.4 ± 1.3 ka
CY02B	87/89	1.01	0.21	58.90 ± 1.34	3.71 ± 0.25	15.9 ± 1.3 ka
CY04A	93/96	1.00	0.17	25.59 ± 0.53	4.09 ± 0.34	6.3 ± 0.6 ka
CY04B	94/96	1.01	0.26	45.86 ± 1.21	3.58 ± 0.34	12.8 ± 1.4 ka
CY04C	93/96	0.99	0.26	47.93 ± 1.39	3.26 ± 0.28	14.7 ± 1.5 ka
CY07A	44/48	1.00	0.20	2.61 ± 0.80	3.51 ± 0.31	750 ± 80 yr
CY07B	- - -	- - -	- - -	- - -	- - -	*no quartz recovered*
EA02	73/91	1.19	**1.16**	*highly dispersed*	- - -	*not suitable*
EA06	45/48	1.05	0.21	4.45 ± 0.14	4.23 ± 0.34	1,050 ± 100 yr

[a]Number of aliquots suitable for age analysis/number of aliquots from which data were collected.
[b]Mean/median ratio; a measure of distribution symmetry (Supplement to Lepper et al. 2007).
[c]Coefficient of variation; relative measure of data dispersion (Fuchs and Wagner 2003).

the colluvial aprons with a northeasterly slope aspect. Additional sedimentological analyses would be required to verify this interpretation and to quantify the eolian contributions to foot-slope development in the study area.

The OSL ages determined in this study indicate that primary accumulation of foot-slope deposits in Cañada del Buey occurred fairly continuously between 15.9 ka and 12.8 ka, possibly with continued inputs until 11.4 ka. These results coincide with a period of colluvial deposition dated in several local canyons between 16.6 ka and 11.8 ka (Phillips et al. 1998; Reneau et al. 1996; Reneau and McDonald 1996). We have dated deposition in the mid-slope of the colluvial apron at 6.3 ka, which corresponds to the middle Holocene altithermal that peaked between 7.5 ka and 5.5 ka (Dean et al. 1996; Meltzer 1999). Alluvial deposition within the Pajarito Plateau canyon systems has also been documented during this time (Reneau et al. 1996; Phillips et al. 1998). Both landscape positions in this study also show evidence of deposition between 1,050 yrs and 750 yrs ago during the so-called "13th century paleomegadrought" (Woodhouse and Overpeck 1998), a climatic event that has been recognized both locally (Drakos et al. 2007) and throughout the Southern Plains with ages ranging from approximately 1,000 yrs to 700 yrs (Madole 1995; Stokes and Swinehart 1997; reviewed in Woodhouse and Overpeck 1998; Lepper and Scott 2005). These observations indicate a strong temporal correlation between eolian inputs into the Pajarito Plateau mesa and canyon systems and colluvial-apron deposition. This, in turn, suggests the importance of the availability of eolian mantling material to remobilization processes such as colluviation and alluviation.

Conclusions

Foot-slope deposits within Cañada del Buey were found to represent a complex interplay of processes in which eolian sediment derived from outside of the Parjarito Plateau plays a role. Based on the results of this study, it can be postulated that eolian inputs contribute, at least to some degree,

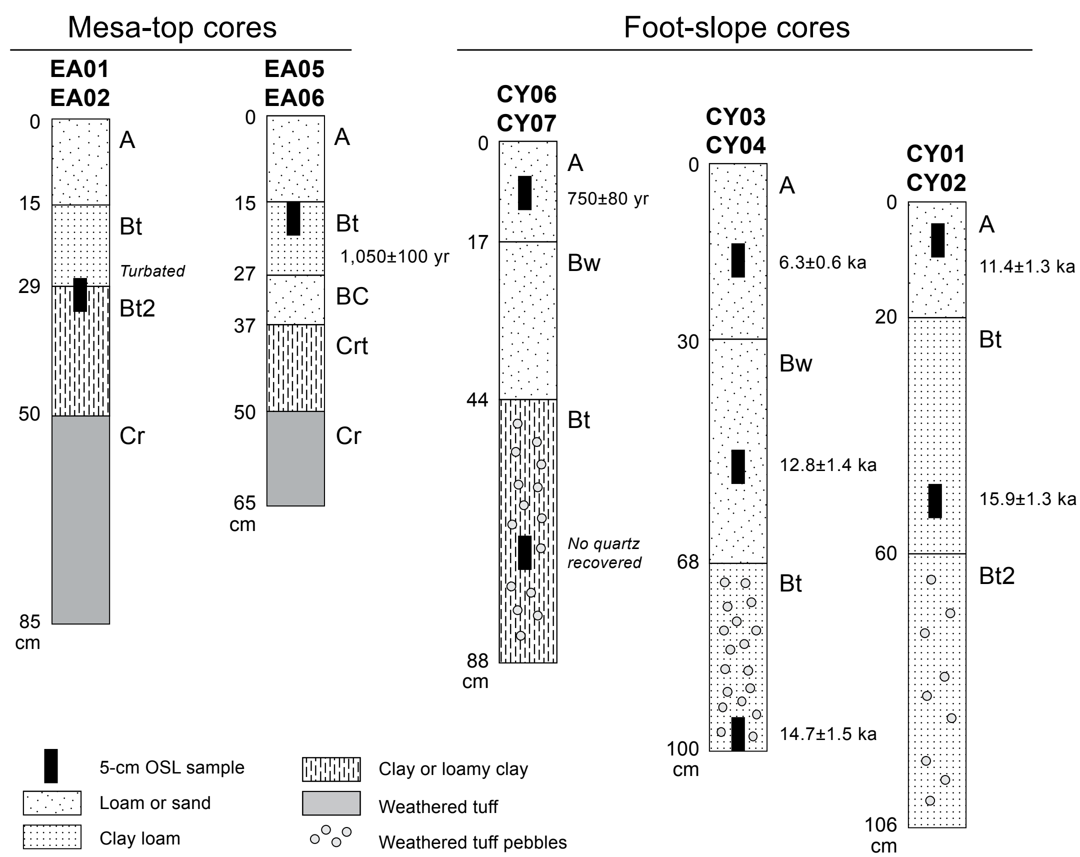

FIGURE 6—Graphical summary of OSL age results combined with soil stratigraphy. Circles within the Bt subhorizons of the foot-slope cores indicate the presence and relative concentration of pebble- and/or gravel-sized weathered tuff fragments.

to the observed geomorphic asymmetry among foot slopes on either side of many mesas on the plateau. Additional work would be required to validate this interpretation. Depositional ages obtained, both from the mesa top and foot slopes, record episodic inputs to the system in the late Pleistocene, middle Holocene, and late Holocene. These periods correlated well to eolian activity and significant climatic events in the Southern Plains and desert Southwest.

Acknowledgments

The authors would like to acknowledge the contributions of Johnny Salazar, Mel Garcia, and Joe Leo Martinez of LANL EES-2 who performed the coring for this project. The work was supported by DOE grant W-7405-ENG-36 032-001-04. INAA was obtained via the DOE Reactor Sharing Grant Program for which the authors would like extend thanks to Mr. Joe Talnagi at The Ohio State University Research Reactor. The authors would also like to recognize and thank Steve Reneau for his valuable input in the form of numerous conversations that helped form a better understanding of the context for the present work. J. B. J. Harrison, L. D. McFadden, and an anonymous reviewer read an earlier version of this manuscript and made suggestions for its improvement. This document has been approved for public release, LA-UR10-07678.

References

Aitken, M. J., 1998, An introduction to optical dating: Oxford University Press, New York, 267 pp.

Broxton, D. E., Heiken, G. H., Chipera, S. J., and Byers, F. M., 1995, Stratigraphy, petrology, and mineralogy of Bandelier Tuff and Cerro Toledo deposits; *in* Broxton, D. E., and Eller, P. G., (eds.), Earth science investigations for environmental restoration—Los Alamos National Laboratory Technical Area 21: Los Alamos National Laboratory, Report LA-12934-MS, pp. 33–63.

Burnett, B. N., Meyer, G. A., and McFadden, L. D., 2008, Aspect-related microclimatic influences on slope forms and processes, northeastern Arizona: Journal of Geophysical Research, v. 113, F03002 18 pp., doi:10.1029/207JF000789.

Bush, D. A., and Feathers, J. K., 2003, Application of OSL single-aliquot and single-grain dating to quartz from anthropogenic soil profiles in the SE United States: Quaternary Science Reviews, v. 22, no. 10–13, pp. 1153–1159.

Carey, J., and Cole, G., 2002, Description of the Cerro Grande fire laser altimetry (LIDAR) data set: Los Alamos National Laboratory, Report LA-13892-MS.

Dean, W. E., Ahlbrandt, T. S., Anderson, R. Y., and Bradbury, J. P., 1996, Regional aridity in North America during the middle Holocene: The Holocene, v. 6, no. 2, pp. 145–155.

Drakos, P. G., and Reneau, S. L., 2007, Episodic eolian events and preservation of mesa top archaeological sites on the Pajarito Plateau, New Mexico; *in* Kues, B. S., Kelley, S. A., and Lueth, V. W. (eds.), Geology of the Jemez region II: New Mexico Geological Society, Guidebook 58, pp. 449–458.

Drakos, P. G., Reneau, S. L., and Morgan, G. S., 2007, *Bison Antiquus* occurrence and Pleistocene–Holocene stratigraphy, Cañada del Buey, Pajarito Plateau, New Mexico; *in* Kues, B. S., Kelley, S. A., and Lueth, V. W. (eds.), Geology of the Jemez region II: New Mexico Geological Society, Guidebook 58, pp. 441–448.

Eberly, P., McFadden, L., and Muir Watt, P., 1995, Eolian dust as a factor in soil development on the Pajarito Plateau, Los Alamos area, northern New Mexico; *in* Goff, F., Kues, B. S., Rogers, M. A., McFadden, L. D., and Gardner, J. N. (eds.), The Jemez Mountains region: New Mexico Geological Society, Guidebook 47, pp. 383–389.

Environmental Surveillance Program, 2003, Air surveillance; *in* Environmental surveillance at Los Alamos during 2003: Los Alamos National Laboratory, Report LA-14162-ENV, pp. 47–92.

Fuchs, M., and Wagner, G. A., 2003, Recognition of insufficient bleaching by small aliquots of quartz for reconstructing soil erosion in Greece: Quaternary Science Reviews, v. 22, pp. 1161–1167.

Gardner, J. N., Reneau, S. L., Lavine, A., Lewis, C. J., Katzman, D., McDonald, E. V., Wilson, J., Goodwin, L., Kelson, K. I., Lepper, K., and Wilson, C. J., 2003, Paleoseismic trenching in the Guaje Mountain fault zone, Pajarito fault system, Rio Grande rift, New Mexico: Los Alamos National Laboratory, Report LA-14087-MS, 68 pp.

Izett, G. A., and Obradovich, J. D., 1994, $^{40}Ar/^{39}Ar$ age constraints for the Jaramillo Normal Subchron and the Matuyama–Brunhes geomagnetic boundary: Journal of Geophysical Research, v. 99, pp. 2925–2934.

Lepper, K., and Scott, G. F., 2005, Late Holocene aeolian activity in the Cimarron River valley of west-central Oklahoma: Geomorphology, v. 70, pp. 42–52.

Lepper, K., Agersnap-Larsen, N., and McKeever, S. W. S., 2000, Equivalent dose distribution analysis of Holocene eolian and fluvial quartz sands from central Oklahoma: Radiation Measurements, v. 32, pp. 603–608.

Lepper, K., Fisher, T., Hajdas, I., and Lowell, T., 2007, Ages for the Big Stone moraine and the oldest beaches of glacial Lake Agassiz: implications for deglaciation chronology: Geology, v. 35, no. 7, pp. 667–670, and supplement.

Lepper, K., Wilson, C., Gardner, J., Reneau, S., and Levine, A., 2003, Comparison of SAR techniques for luminescence dating of sediments derived from volcanic tuff: Quaternary Science Reviews, v. 22, pp. 1131–1138.

Madole, R. F., 1995, Spatial and temporal patterns of late Quaternary eolian deposition, eastern Colorado, USA: Quaternary Science Reviews, v. 14, pp. 155–177.

Meltzer, D., 1999, Human responses to middle Holocene (Altithermal) climates on the North American Great Plains: Quaternary Research, v. 52, pp. 404–416.

Murray, A. S., and Wintle A. G., 2000, Luminescence dating of quartz using an improved single-aliquot regenerative-dose protocol: Radiation Measurements, v. 32, pp. 57–73.

Phillips, E. H., Goff, F., Kyle, P. R., McIntosh, W. C., Dunbar, N. W., and Gardner, J. N., 2007, The $^{40}Ar/^{39}Ar$ age constraints on the duration of resurgence at the Valles caldera, New Mexico: Journal of Geophysical Research, v. 112, B08201, doi:10.1029/2006JB004511.

Phillips, W., McDonald, E., Reneau, S., and Poths, J., 1998, Dating soils and alluvium with cosmogenic ^{21}Ne depth profile: case studies from the Pajarito Plateau, New Mexico, USA: Earth and Planetary Science Letters, v. 160, pp. 209–213.

Prescott, J. R., and Hutton, J. T., 1988, Cosmic ray and gamma ray dosimetry for TL and ESR: Nuclear Tracks and Radiation Measurement, v. 14, pp. 223–227.

Prescott, J. R., and Hutton, J. T., 1994, Cosmic ray contributions to dose rates for luminescence and ESR dating: large depths and long-term time variations: Radiation Measurements, v. 23, pp. 497–500.

Reneau, S. L., 1995, Geomorphic studies at DP mesa and vicinity; *in* Broxton, D. E., and Eller, P. G. (eds.), Earth science investigations for environmental restoration—Los Alamos National Laboratory Technical Area 21: Los Alamos National Laboratory, Report LA-12934-MS, pp. 65–92.

Reneau, S. L., and McDonald, E. V., 1996, Landscape history and processes on the Pajarito Plateau, northern New Mexico: Rocky Mountain Cell, Friends of the Pleistocene, Field Trip Guidebook; Los Alamos National Laboratory, Report LA-UR-96-3035, 195 pp.

Reneau, S. L., Kolbe, T., Simpson, D., Carney, J. S., Gardner, J. N., Olig, S. S., and Vaniman, D. T., 1995, Surficial materials and structure at Pajarito Mesa; *in* Reneau, S .L., and Raymond, R., Jr. (eds.), Geological site characterization for the proposed Mixed Waste Disposal Facility, Los Alamos National Laboratory: Los Alamos National Laboratory, Report LA-13089-MS, pp. 31–69.

Reneau, S. L., McDonald, E. V., Gardner, J. N., Kolbe, T. R., Carney, J. S., Watt, P. M., and Longmire, P. A., 1996, Erosion and deposition on the Pajarito Plateau, New Mexico, and implications for geomorphic responses to late Quaternary climatic changes; *in* Goff, F., Kues, B. S., Rogers, M. A., McFadden, L. D., and Gardner, J. N. (eds.), The Jemez Mountains region: New Mexico Geological Society, Guidebook 47, pp. 391–397.

Rowland, J. C., Lepper, K., Dietrich, W. E., Wilson, C. J., and Sheldon, R., 2005, Tie channel sedimentation rates, oxbow formation age and channel migration rate from optically stimulated luminescence (OSL) analysis of floodplain deposits: Earth Surface Processes and Landforms, v. 30, pp. 1161–1179.

Stokes, S., and Swinehart, J., 1997, Middle- and late-Holocene dune reactivation in the Nebraska Sand Hills, USA: The Holocene, v. 7, no. 3, pp. 263–272.

Wintle, A.G., and Murray, A. S., 2006, A review of quartz optically stimulated luminescence characteristics and their relevance in single-aliquot regeneration dating protocols: Radiation Measurements, v. 41, pp. 369–391.

Woodhouse, C. A., and Overpeck, J. T., 1998, 2000 years of drought variability in the central United States: Bulletin of the American Meteorological Society, v. 79, no. 12, pp. 2693–2714.